Supplementary Materials (Duault *et al*.)

Activated Natural Killer Cells Predict Poor Clinical Prognosis in High-risk B- and T- cell Acute Lymphoblastic Leukemia

Inventory

- Supplementary Figures S1-S14
- Supplementary Tables S1-S5

Figure S1: *Manual gating strategy for CyTOF analysis of BMMC and PBMC*

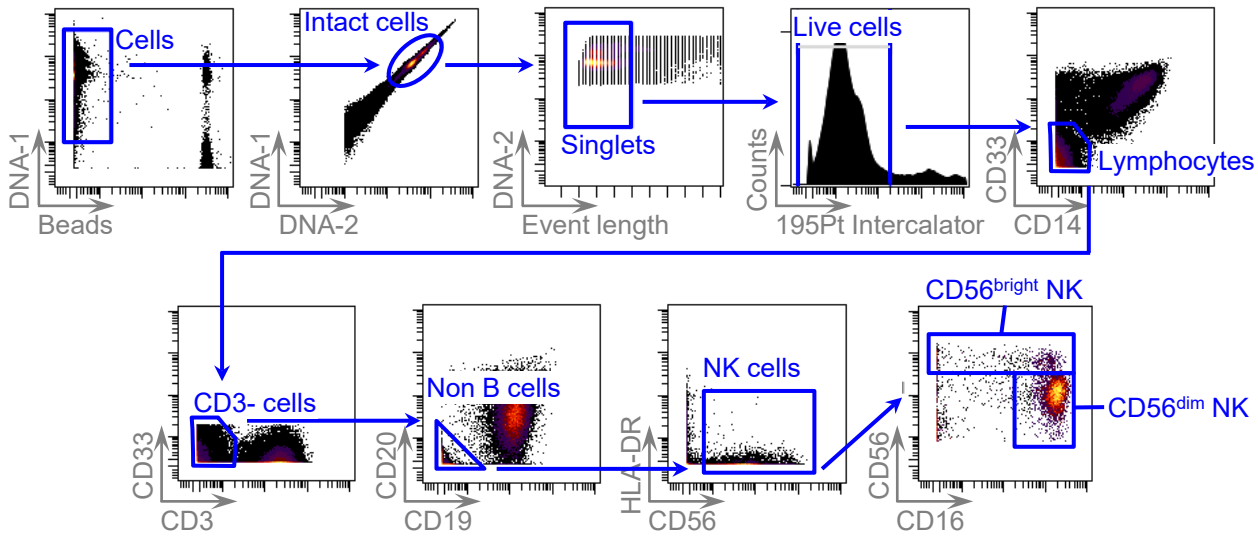

Figure S1: Manual gating strategy for CyTOF analysis of BMMC and PBMC. From the live intact singlet population, NK cells were gated as non-monocyte (Lymphocytes gate), non-T cell (CD3- cells gate), non-B cell (Non B cells gate), $CD56^{+}$ HLA-DR^{-} cells, and then subdivided in $CD56^{bright}$ and $CD56^{dim}$ NK cells according to their surface expression of CD56 and CD16.

Figure S2: *Increased cell death and reduced proliferation are not responsible for reduced NK frequencies in the B/T-ALL microenvironment*

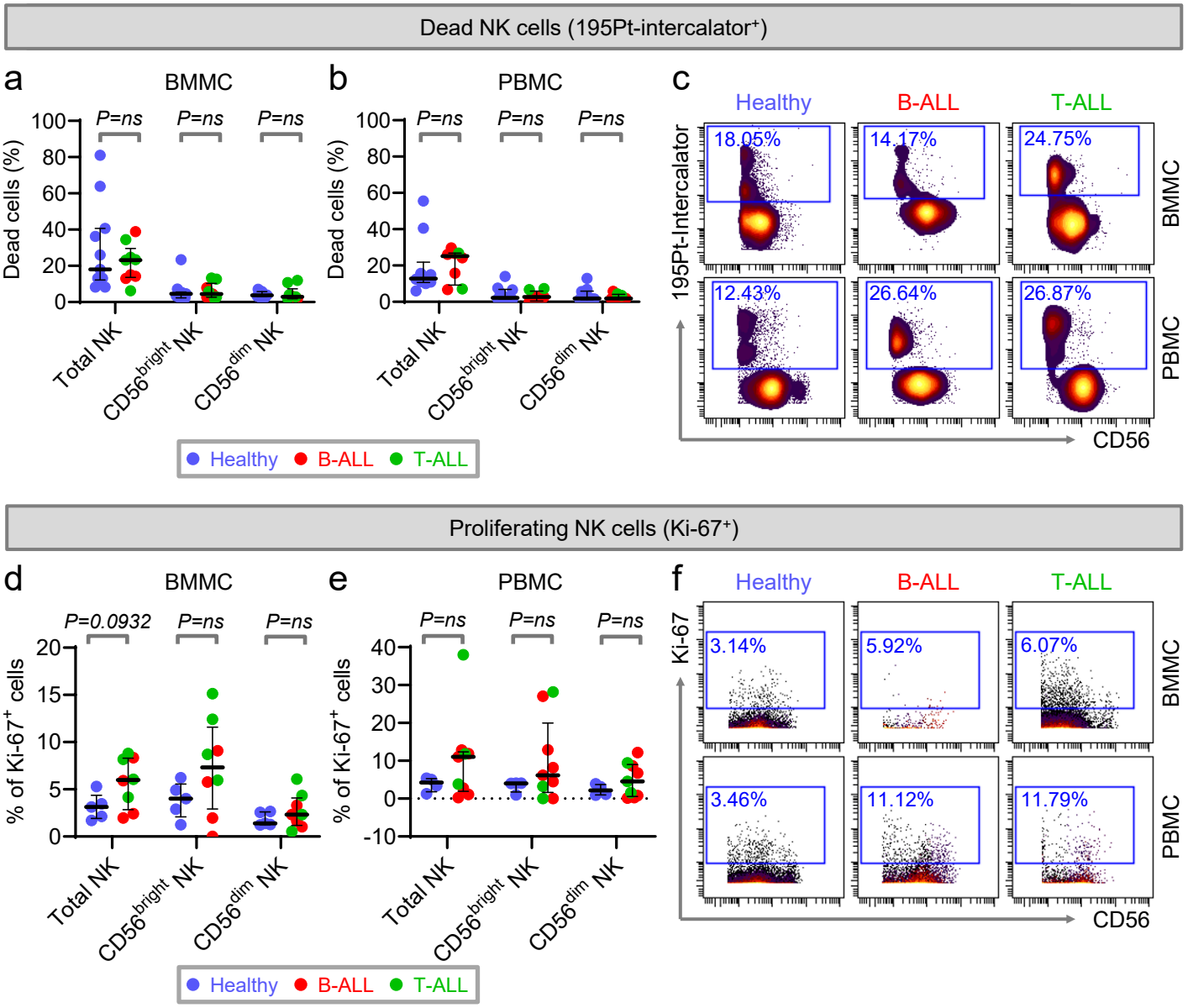

Figure S2: Increased cell death and reduced proliferation are not responsible for reduced NK frequencies in the B/T-ALL microenvironment. (**a-c**) Proportion of dead cells in Total NK cells and NK subsets in BMMC (**a**), and PBMC (**b**), and representative dot plots (**c**), of healthy donors (n=11 BMMC, n=10 PBMC) and B/T-ALL patients (n=9 BMMC, n=8 PBMC) calculated by CyTOF. (**d-f**) Proportion of Ki-67$^+$ proliferating total NK cells and NK subsets in BMMC (**d**), and PBMC (**e**), and representative dot plots (**f**), of healthy donors (n=5 BMMC, n=4 PBMC) and B/T-ALL patients (n=8 BMMC, n=9 PBMC) calculated by CyTOF. Graphs show median ± interquartile range. Exact p-values have been calculated using the Mann-Whitney test, ns=non-significant.

Figure S3: *Purity assessment of sorted NK cells from healthy donors and B/T-ALL patients*

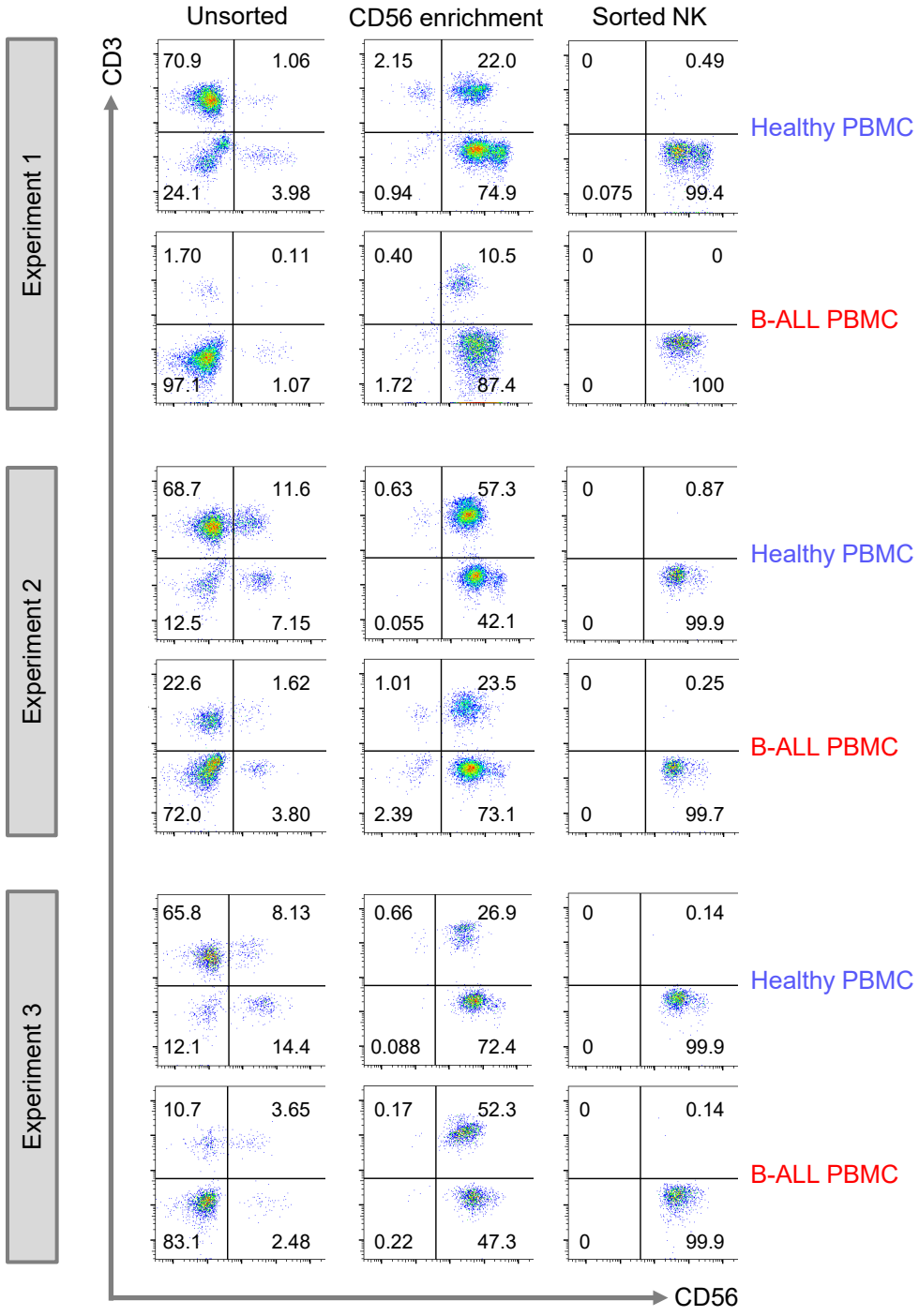

Figure S3: Purity assessment of sorted NK cells from healthy donors and B/T-ALL patients. Flow cytometry dot plots showing percentages of NK cells in PBMC of healthy donors (n=3) and B/T-ALL patients (n=3) before sorting (unsorted), after separation of total $CD56^+$ cells using release CD56 microbeads (CD56 enrichment), and after automated cell sorting of CD56-enriched cells to obtain $CD3^-$ $CD56^+$ NK cells (sorted NK).

Figure S4: *Differentially regulated genes between CD56^{bright} and CD56^{dim} NK subsets (GSE21774)*

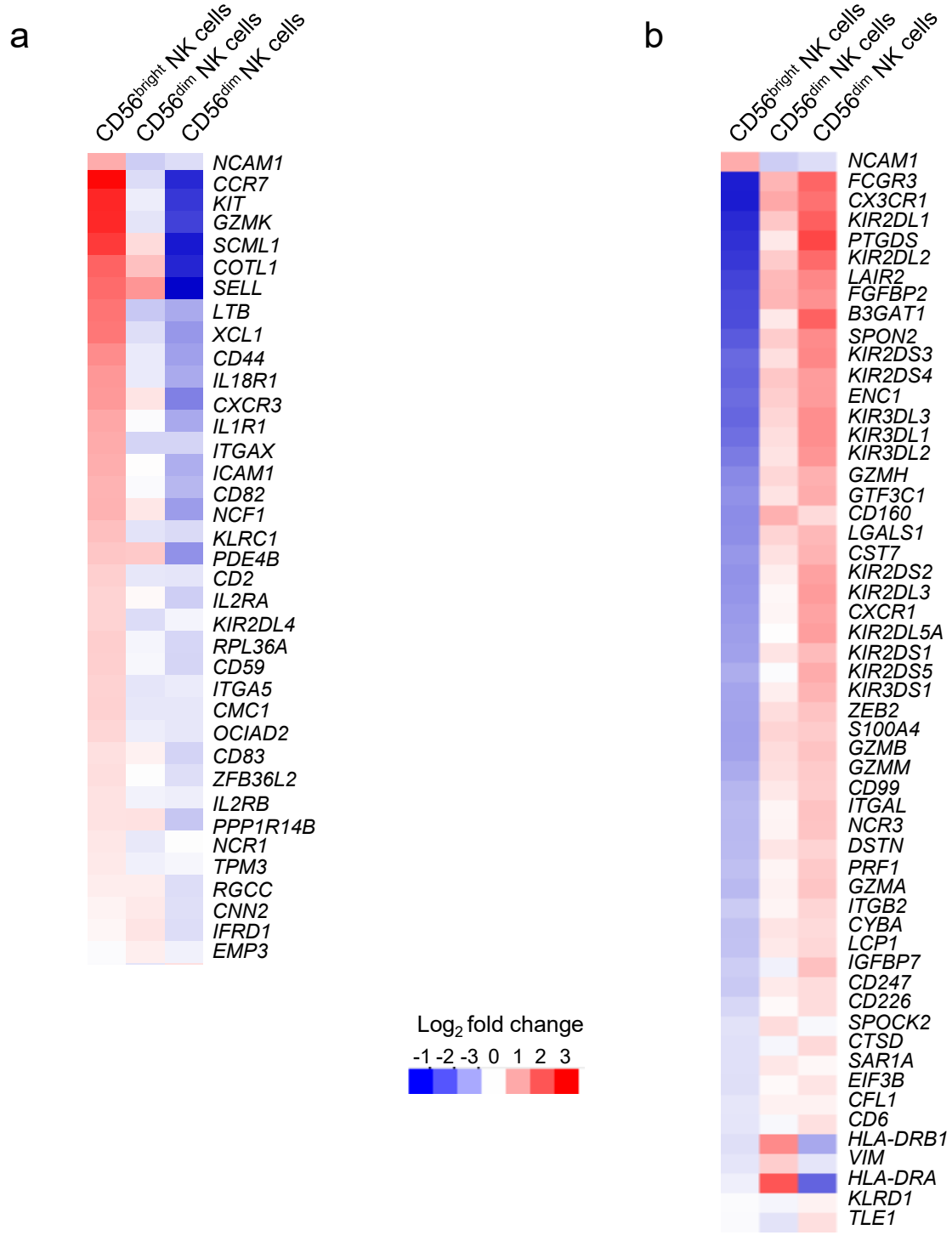

Figure S4: Differentially regulated genes between CD56^{bright} and CD56^{dim} NK subsets (GSE21774). (**a-b**) Heatmaps depicting selected well-known differentially regulated genes between CD56^{bright} and CD56^{dim} NK subsets in the GSE21774 reference matrix used in CIBERSORT in Figs. 2a-b.

Figure S5: *Changes in frequencies of CD56^{bright} and CD56^{dim} NK cells in high-risk B/T-ALL*

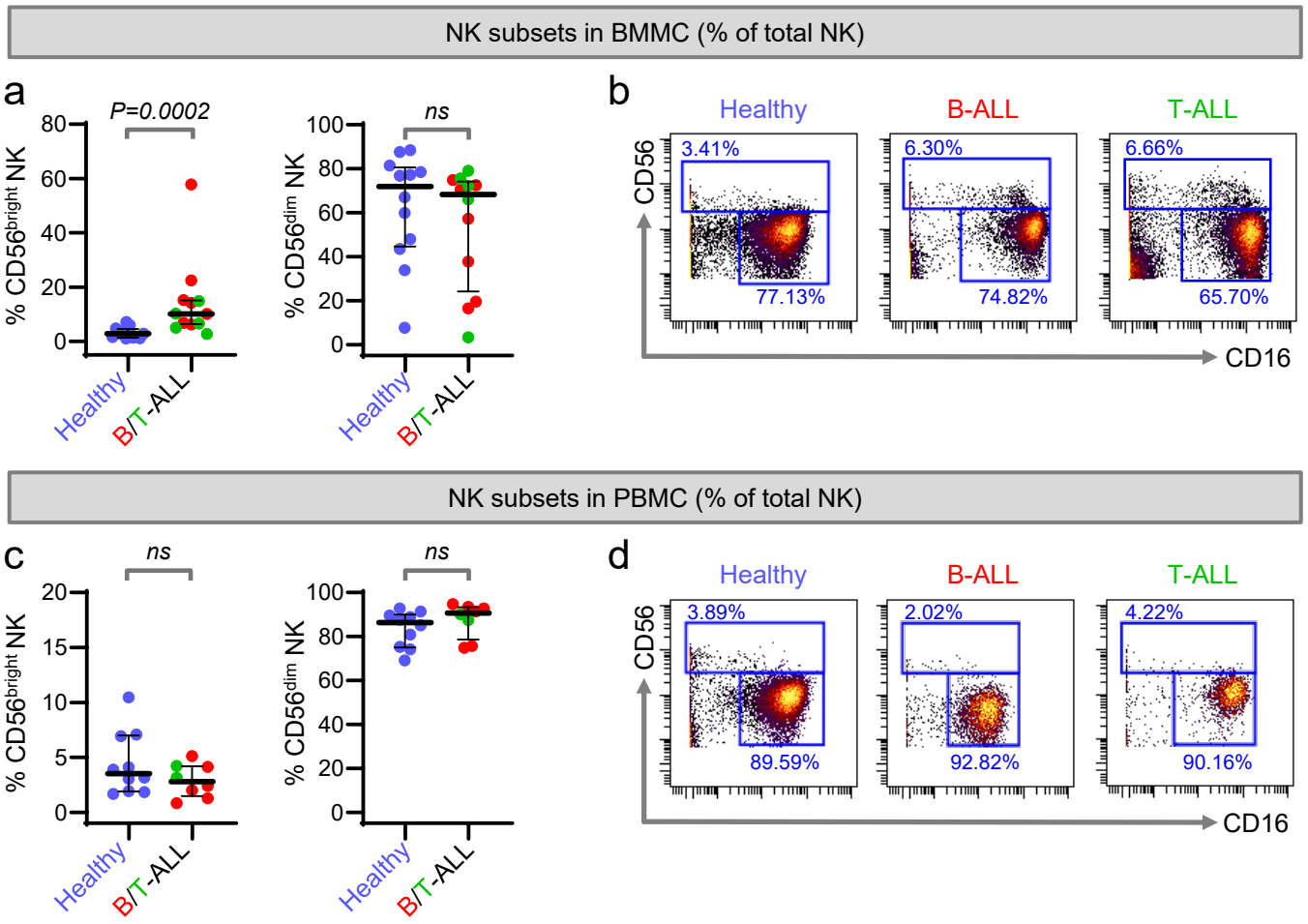

Figure S5: Changes in frequencies of CD56^{bright} and CD56^{dim} NK cells in high-risk B/T-ALL. (a-b) Comparison of percentages (**a**), and representative dot plots (**b**) of CD56^{bright} NK and CD56^{dim} NK cells in BMMC of healthy donors (n=12) and B/T-ALL patients (n=12) by CyTOF. **(c-d)** Comparison of percentages (**c**), and representative dot plots (**d**) of CD56^{bright} NK, and CD56^{dim} NK cells in PBMC of healthy donors (n=10) and B/T-ALL patients (n=8). All NK subsets are shown as percentages of total NK cells. Graphs show median ± interquartile range. Exact p-values were calculated using the Mann-Whitney test. ns = non-significant.

Figure S6: *Changes in NKp46, CD27, and CD57 expression in unstimulated NK cells between B/T-ALL patients and healthy donors*

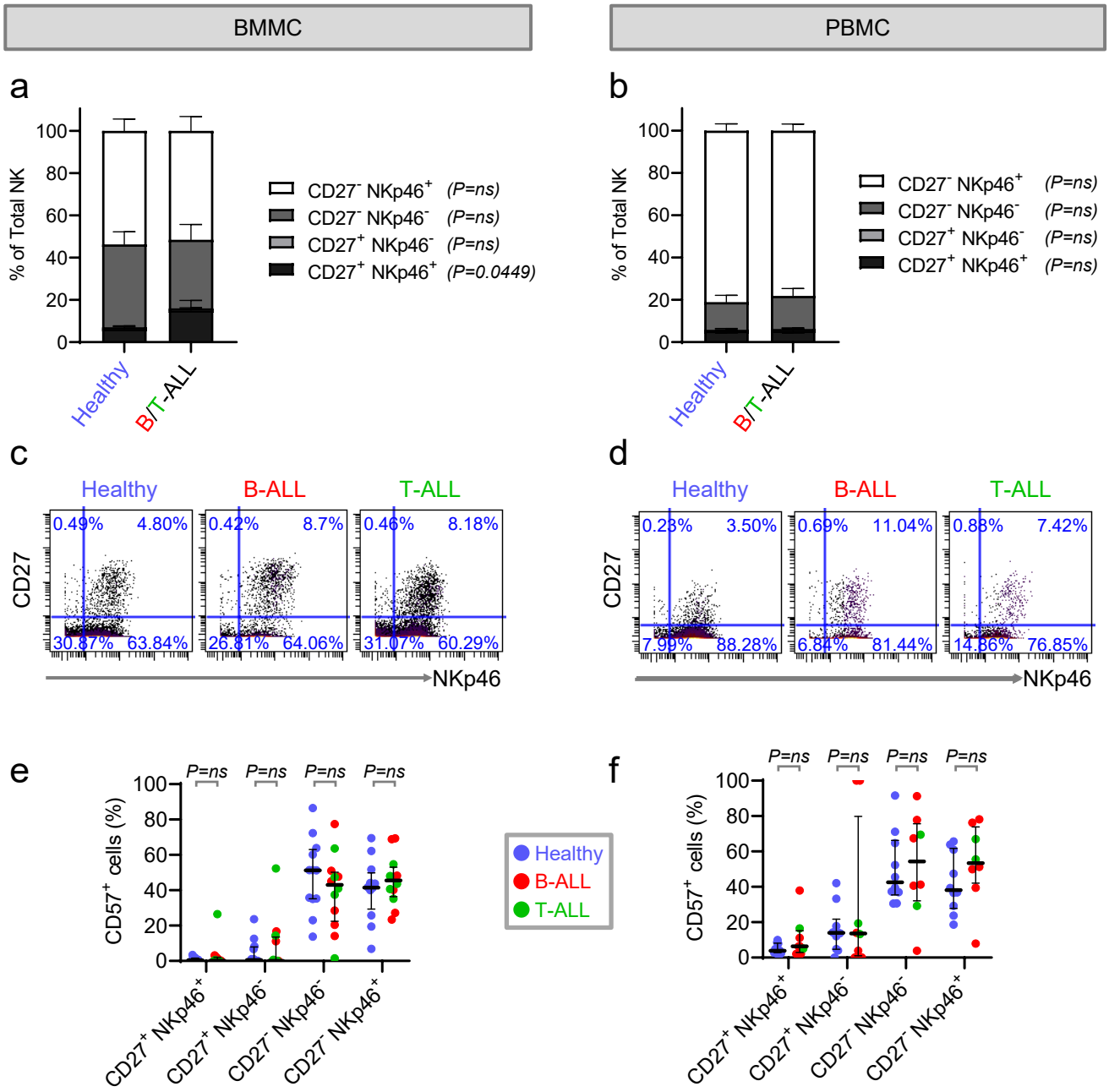

Figure S6: Changes in NKp46, CD27 and CD57 expression in unstimulated NK cells between B/T-ALL patients and healthy donors. (**a-b**) CD27 *vs* NKp46 expression analysis by CyTOF in total NK cells of BMMC (**a**) and PBMC (**b**) of B/T-ALL patients (BMMC, n=12; PBMC, n=8) compared to healthy individuals (BMMC, n=12; PBMC, n=10). Graphs show mean + SEM for each subset. (**c-d**) Representative dot plots of the expression of CD27 *vs* NKp46 on total NK cells in BMMC (**c**) and PBMC (**d**) of healthy control and B/T-ALL patients. (**e-f**) CD57 expression on subsets defined by CD27 and NKp46 expression as described in (a-b). Graphs show median ± interquartile range. Exact p-values were calculated using the Mann-Whitney test, ns= not significant.

Figure S7: *Gating strategy for flow cytometry analysis of PBMC*

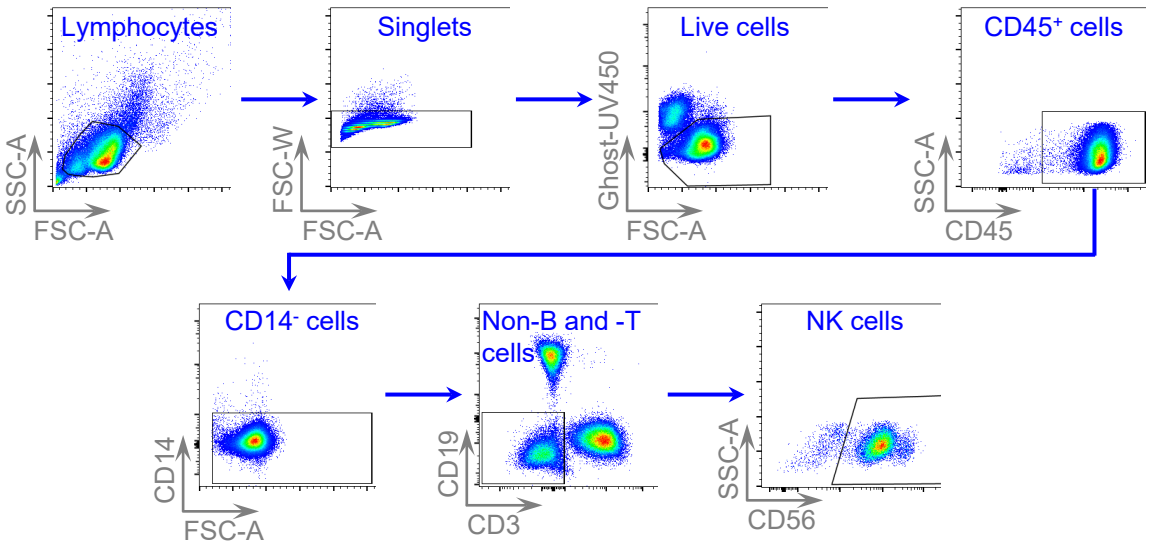

Figure S7: Gating strategy for flow cytometry analysis of PBMC. From the lymphocyte cluster; singlets were gated followed by selection of live (Ghost-UV450^{-}) and CD45^{+} populations. Monocytes were then gated out (CD14^{-} gate), followed by the non-B and non-T cell gate (CD19^{-}CD3^{-}). From non-B non-T and non-monocyte populations, CD56^{+} NK cells were selected for downstream gating of surface markers.

Figure S8: *Cytokine production in stimulated BMMC and PBMC NK cells of B/T-ALL patients*

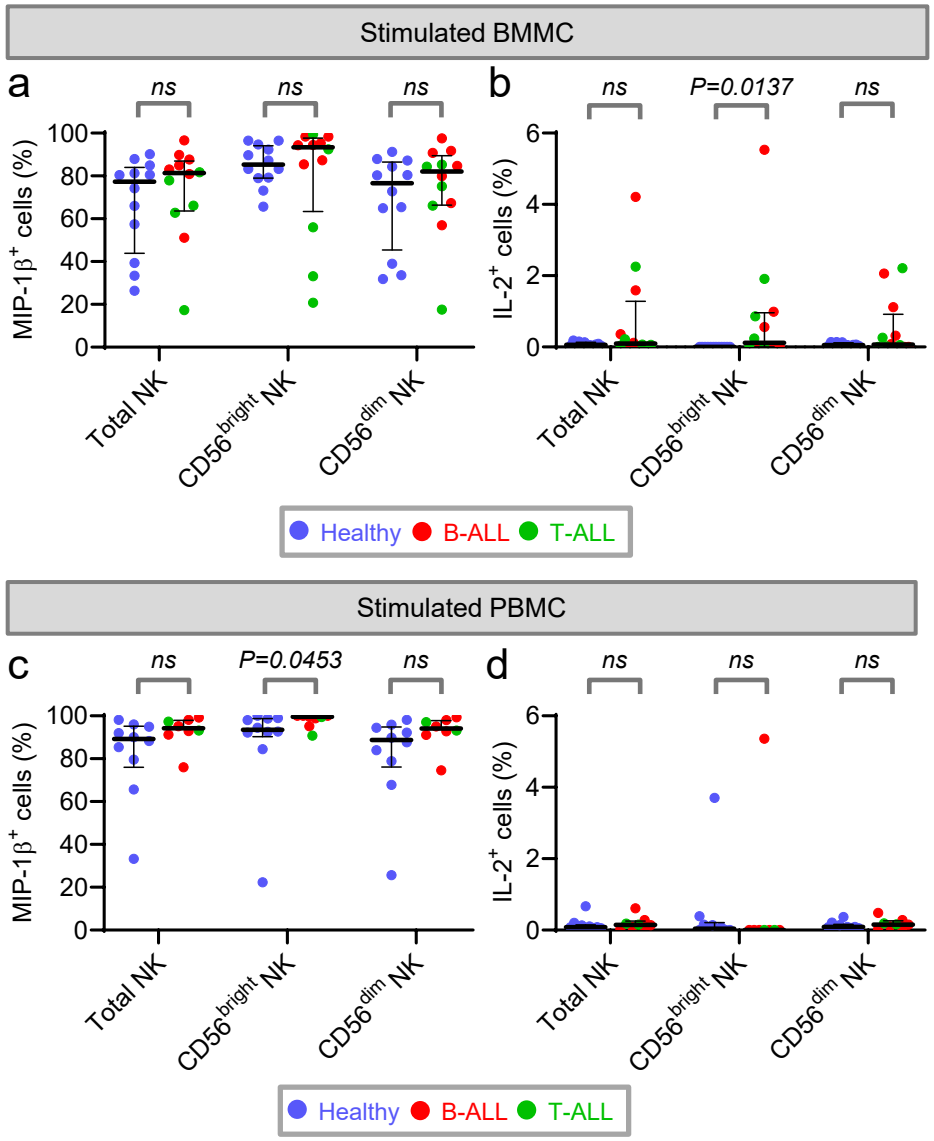

Figure S8: Cytokine production in stimulated BMMC and PBMC NK cells of B/T-ALL patients. (**a-d**) Frequencies of PMA/Ionomycin-stimulated cells expressing MIP-1β (**a,c**) and IL-2 (**b,d**) in total NK and NK subsets in BMMC (**a-b**) and PBMC (**c-d**) of B/T-ALL patients (BMMC, n=12; PBMC, n=8) and healthy donors (BMMC, n=12; PBMC, n=10). (**e-f**) Representative dot plots for stimulated total NK cells expressing MIP-1β and IL-2 in BMMC (**e**) and PBMC (**f**) of B/T-ALL patients. Graphs show median± interquartile range. Exact p-values were calculated using Mann-Whitney test, ns = not significant.

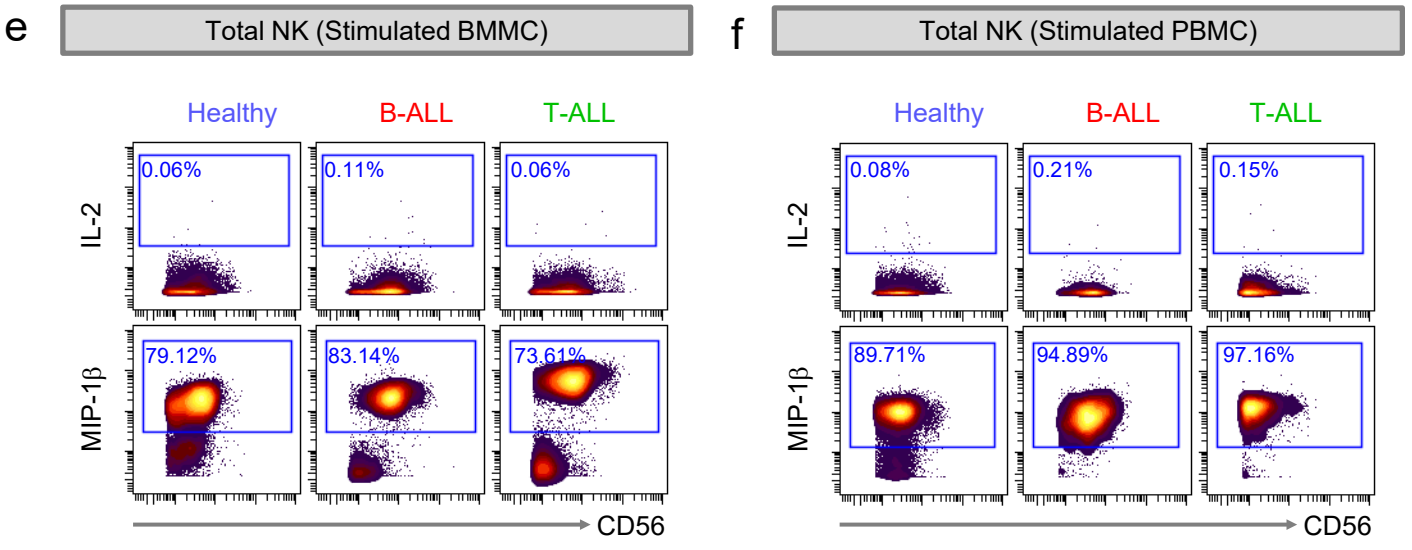

Figure S9: *Comparison of cytotoxic granules and degranulation of NK cells between B/T-ALL patients and healthy donors*

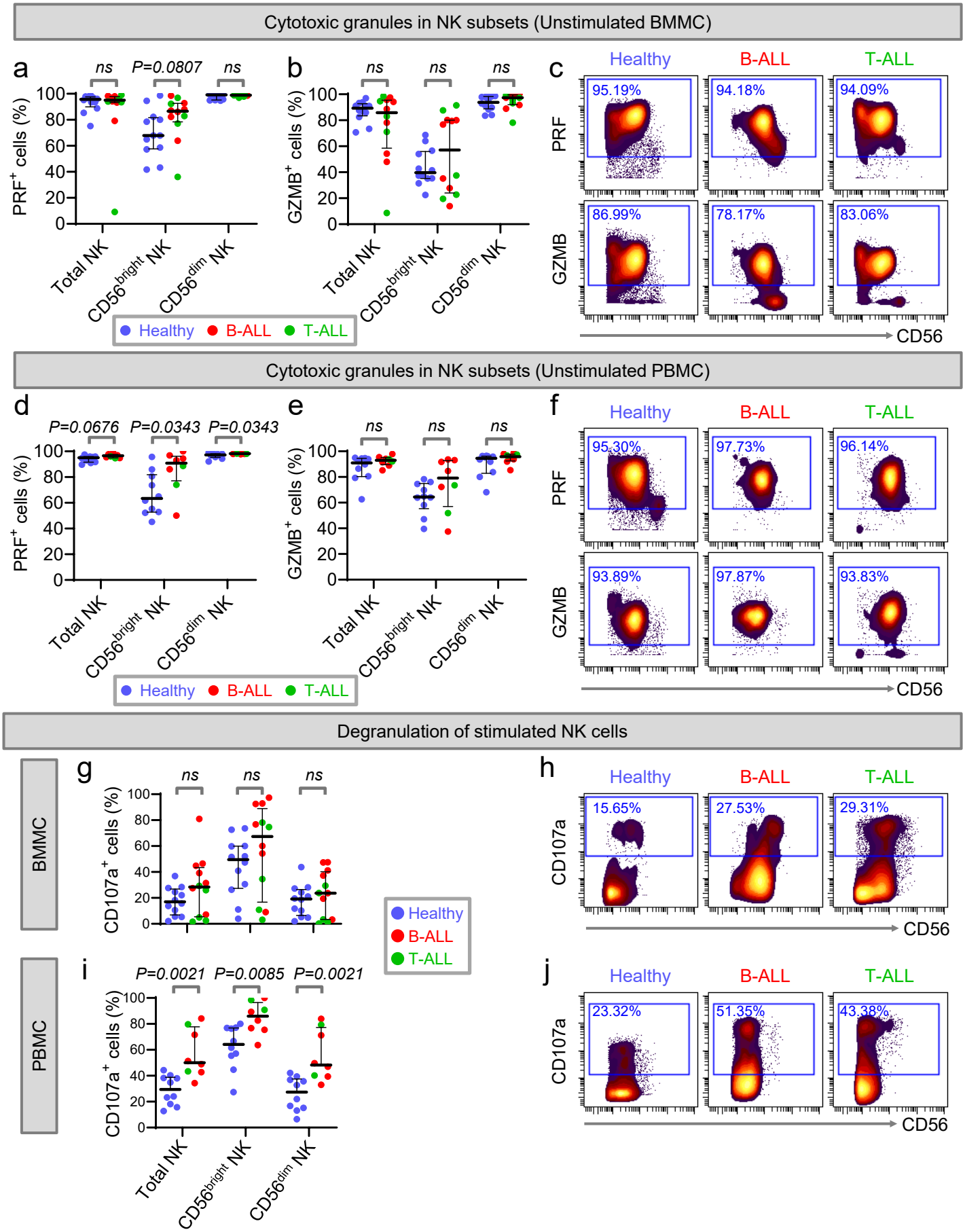

Figure S9: Comparison of cytotoxic granules and degranulation of NK cells between B/T-ALL patients and healthy donors. (**a-b**) Frequencies of cells expressing perforin (PRF, (**a**)) and granzyme B (GZMB, (**b**)) in unstimulated total NK cells and NK subsets in BMMC of B/T-ALL patients (n=12) and heathy donors (n=12). (**c**) Representative density plots showing PRF and GZMB *vs* CD56 expression in unstimulated total NK cells in BMMC of B/T-ALL patients and heathy donors. (**d-e**) Frequencies of cells expressing PRF (**d**) and GZMB (**e**) in unstimulated total NK cells and NK subsets in PBMC of B/T-ALL patients (n=8) and heathy donors (n=10). (**f**) Representative density plots showing PRF and GZMB *vs* CD56 expression in unstimulated total NK cells in PBMC of B/T-ALL patients and heathy donors. (**g-j**) Comparison of frequencies (**g, i**) and representative density plots (**h, j**) of PMA/Ionomycin-stimulated NK cell subsets expressing CD107a in BMMC (**g-h**) and PBMC (**i-j**) of healthy donors (BMMC: n=12, PBMC: n=10) and B/T-ALL patients (BMMC: n=12, PBMC: n=8) by CyTOF. Graphs show median ± interquartile range. Exact p-values were calculated using Mann-Whitney test, ns=not significant.

Figure S10: *Comparison of expression of immune checkpoints in BMMC of ALL patients and healthy donors*

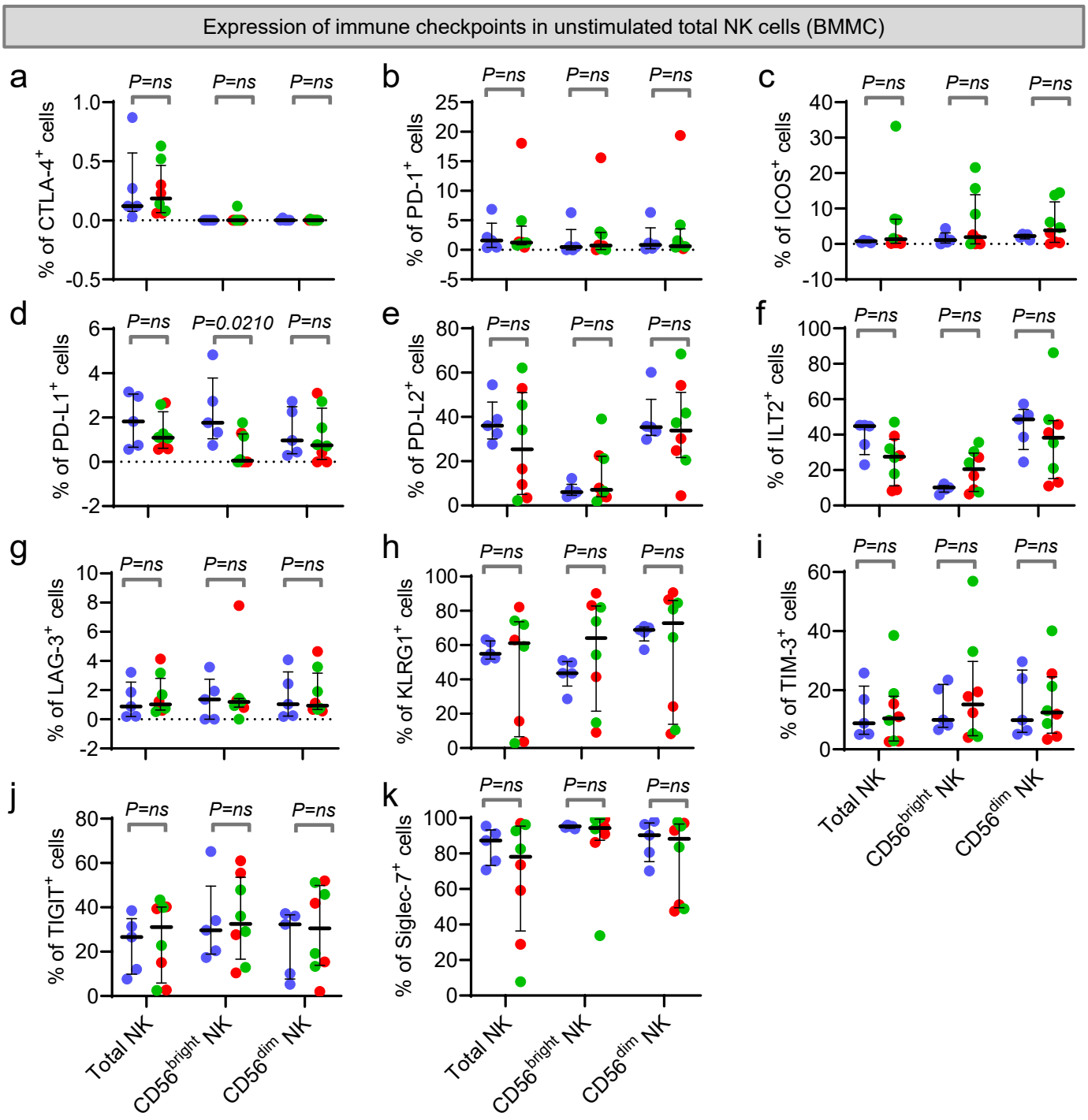

Figure S10: Comparison of expression of immune checkpoints in BMMC of ALL patients and healthy donors. (**a-k**) Comparison of the proportions of total NK cells or CD56^{bright}, CD56^{dim} NK subsets expressing CTLA-4 (**a**) , PD-1 (**b**) , ICOS (**c**), PD-L1 (**d**), PD-L2 (**e**), ILT2 (**f**), LAG-3 (**g**), KLRG1 (**h**), TIM-3 (**i**), TIGIT (**j**), and Siglec-7 (**k**) in healthy donors (n=5) and B/T-ALL patients (n=8) by CyTOF. Graphs show median ± interquartile range. Exact p-values were calculated using Mann-Whitney test, ns=not significant.

Figure S11: *Comparison of expression of immune checkpoints in PBMC of ALL patients and healthy donors*

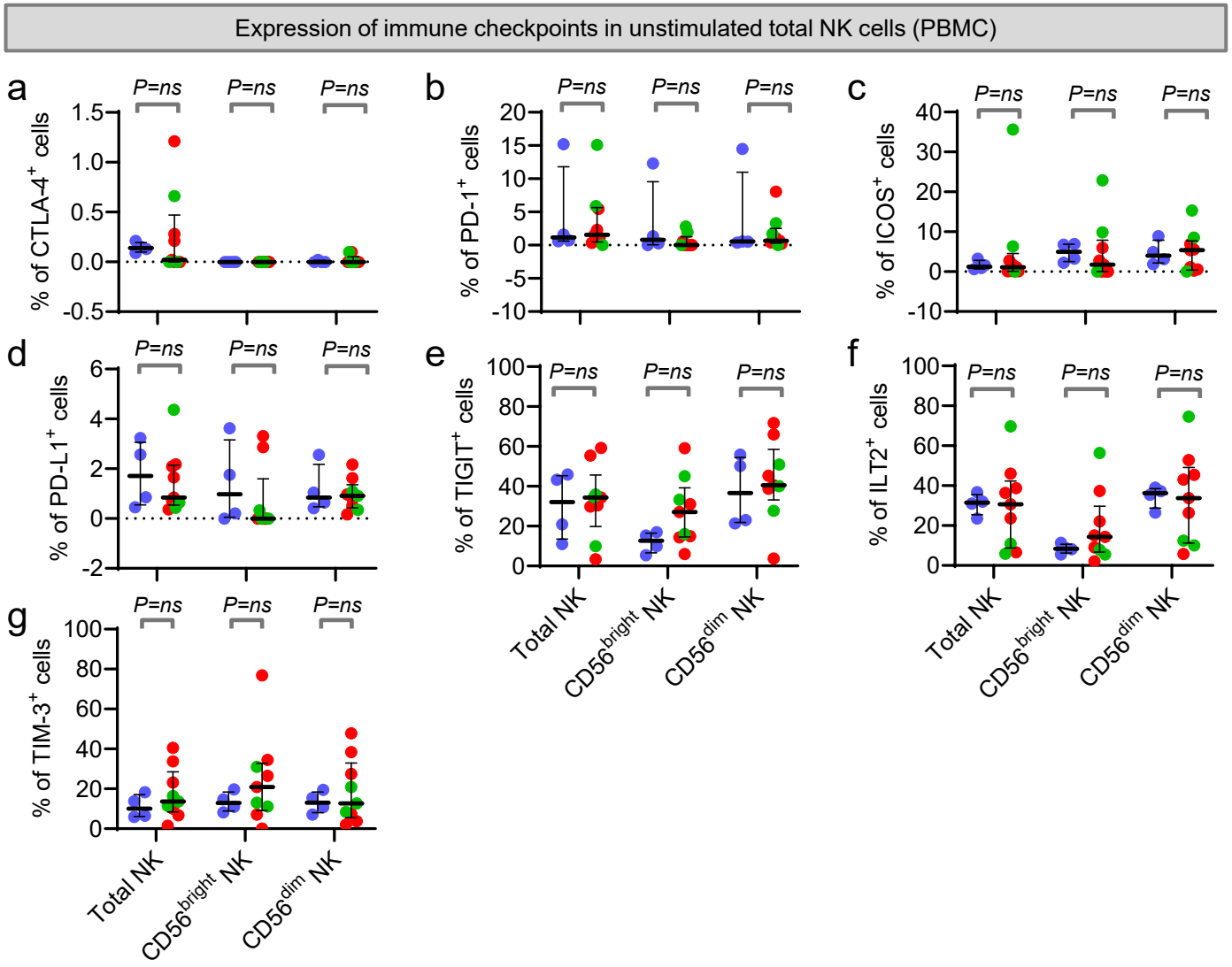

Figure S11: Comparison of expression of immune checkpoints in PBMC of ALL patients and healthy donors. (**a-g**) Comparison of the proportions of Total NK cells or CD56^{bright}, CD56^{dim} NK subsets expressing CTLA-4 (**a**), PD-1 (**b**), ICOS (**c**), PD-L1 (**d**), TIGIT (**e**) , ILT2 (**f**), and TIM-3 (**g**) in healthy donors (n=4) and B/T-ALL patients (n=9) by CyTOF. Graphs show median ± interquartile range. Exact p-values were calculated using Mann-Whitney test, ns=not significant.

Figure S12: *Gene expression signature of resting and activated NK subsets in LM22 CIBERSORT reference matrix*

a

Up regulated genes in Resting NK Cells (more than 2-fold change)							
CHST15	2.00	MNDA	2.62	AZU1	3.46	P2RY13	5.56
BEND5	2.00	IGKC	2.66	ZFP36L2	3.47	LILRB2	5.58
CD2	2.01	PLEKHG3	2.69	SELL	3.60	CHI3L1	5.77
ADAM28	2.05	ZAP70	2.69	CD160	3.63	DENND5B	5.83
ATHL1	2.05	PBXIP1	2.70	PIK3IP1	3.72	RNASE6	5.88
HCK	2.12	TCF7	2.73	FCN1	3.81	CEACAM8	5.89
CLC	2.14	CDH12	2.78	LIME1	3.82	LAG3	5.95
CD3G	2.15	CLEC2D	2.84	CRISP3	3.92	HIST1H2BG	6.09
PPBP	2.16	LRMP	2.85	ZBP1	3.93	PDE6C	6.23
PPFIBP1	2.22	NCF2	2.86	FLJ13197	3.98	CCDC102B	6.53
C1orf54	2.22	RNASE2	2.88	DHX58	4.27	MGAM	6.57
MBL2	2.23	CTSG	2.93	TTC38	4.37	CD68	6.73
KLRC3	2.24	TLR7	2.93	ELANE	4.37	HK3	6.86
FAM65B	2.27	ABCB4	3.00	HTR2B	4.45	AQP9	7.43
LST1	2.31	ARHGAP22	3.00	PADI4	4.45	SEC31B	8.01
VNN1	2.31	ALOX15	3.08	VNN2	4.48	CDHR1	8.03
FAM198B	2.31	MS4A3	3.10	AIF1	4.56	GZMK	8.41
KLRB1	2.32	GUSBP11	3.16	RPL3P7	4.65	GPR1	9.25
HIST1H2AE	2.39	CD72	3.20	CFP	4.86	LY9	9.54
MMP9	2.42	MXD1	3.21	S100A12	4.93	CDA	12.04
CLCA3P	2.43	RASA3	3.25	BPI	5.04	CAMP	12.7
TRAV9-2	2.54	PGLYRP1	3.26	RASGRP2	5.31	DEFA4	14.02
CSF3R	2.55	S1PR5	3.34	FAIM3	5.32	NME8	18.89
MYB	2.61	IL7R	3.39	VILL	5.41	DPEP2	28.70
LILRA2	2.61	CXCR2	3.43	FFAR2	5.50		

Up regulated genes in Activated NK Cells (more than 2-fold change)					
LTA	0.008	RRP12	0.27	CRTAM	0.40
OSM	0.013	TNFRSF4	0.28	SEPT8	0.40
APOL6	0.03	RRP9	0.28	CCR5	0.40
SOCS1	0.04	CCL4	0.28	ARRB1	0.41
LTB	0.05	RCAN3	0.29	SKA1	0.41
CSF2	0.06	CXCL9	0.31	GPR171	0.42
IL2RA	0.06	**CD69**	0.32	TARDBPP1	0.43
IFNG	0.07	MMP25	0.32	KIR2DL1	0.43
CDC25A	0.09	MICAL3	0.33	SAMSN1	0.44
CDK6	0.09	CCL22	0.34	TREML2	0.44
DPP4	0.10	KIR2DL4	0.35	RSAD2	0.45
EGR2	0.11	ANGPT4	0.35	DCSTAMP	0.46
CXCL10	0.13	HIC1	0.37	NCR3	0.46
ORC1	0.14	CCR6	0.38	IL3	0.47
CXCL11	0.15	IL12RB2	0.38	ST8SIA1	0.47
SPAG4	0.16	KIR2DS4	0.38	CCL18	0.49
TNFSF14	0.17	CCL1	0.38		
CCND2	0.17	CR2	0.39		
BIRC3	0.24	FBXL8	0.39		

b

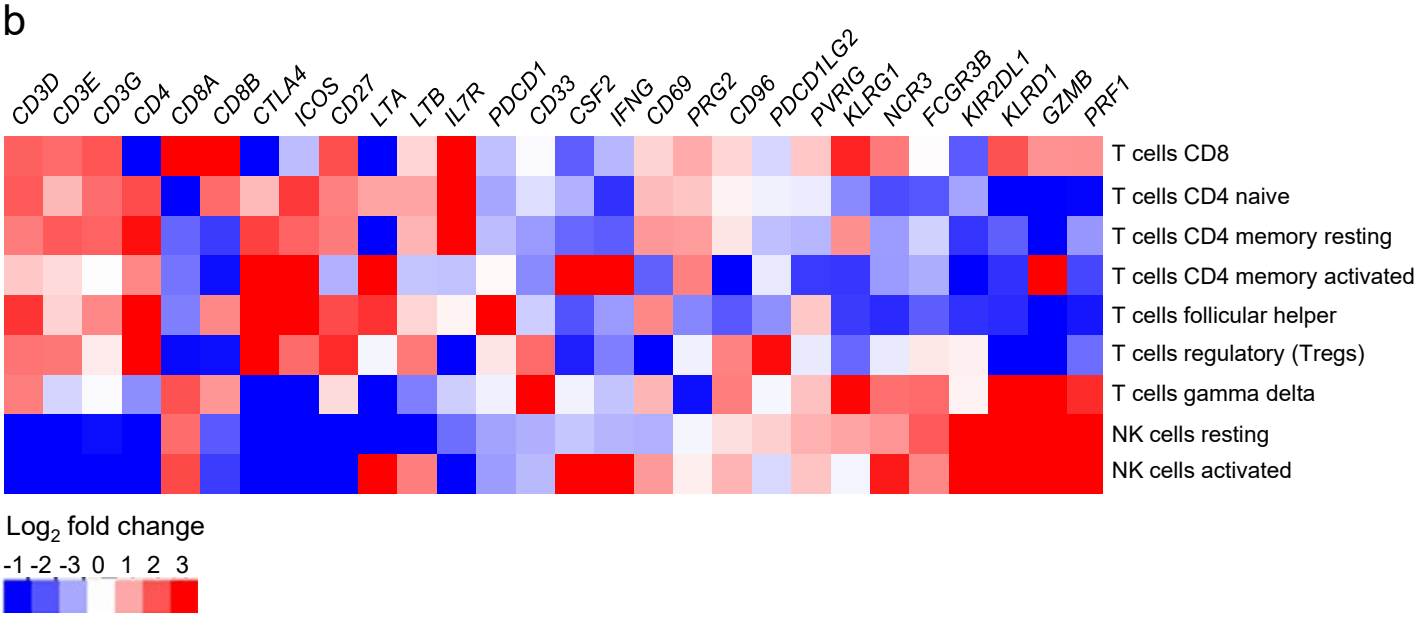

Figure S12: Gene expression signature of resting and activated NK subsets in LM22 CIBERSORT reference matrix. (**a**) List of differentially regulated genes (≥2-fold) between resting and activated NK subsets in LM22 reference matrix used for CIBERSORT to deconvolute COG B-ALL data in Fig.6. (**b**) Heatmap showing that CIBERSORT LM22 matrix uses expression of lineage markers (e.g., CD3, CD4, CD8) to distinguish between T cells and NK cells.

Figure S13: *Poorly prognostic ALL patients with only activated NK cells exhibit chronic NK activation*

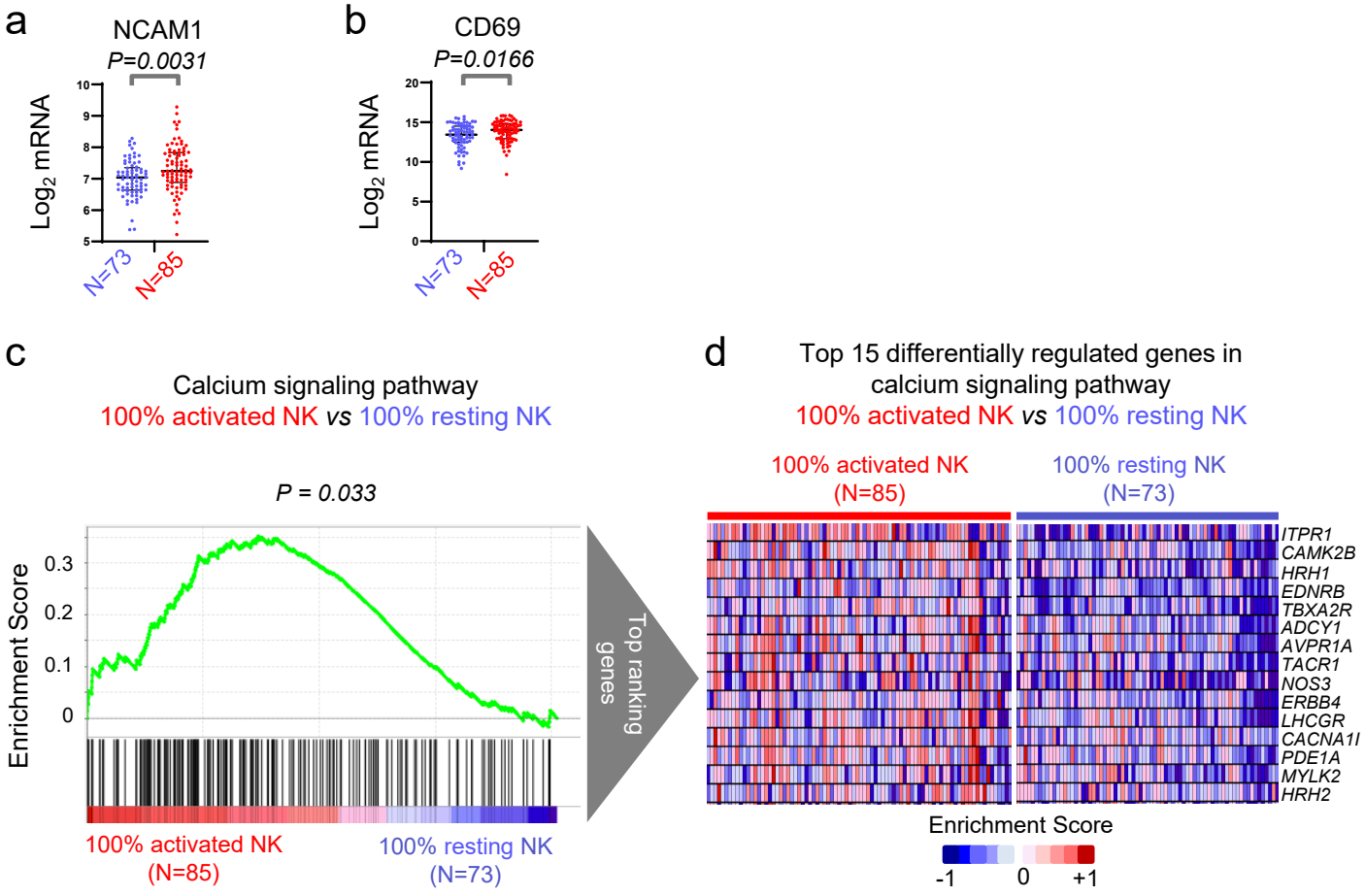

Figure S13: Poorly prognostic ALL patients with only activated NK cells exhibit chronic NK activation. (**a-b**) Comparison of transcript levels of CD56 (**a**) and CD69 NK activation marker (**b**) between COG P9906 B-ALL patients with only activated NK (n=85) or only resting NK (n=73) cells. Exact p-values were calculated using Mann-Whitney test. (**c-d**) Gene set enrichment analysis (GSEA) showing differential regulation of the calcium (Ca^{2+}) signaling pathway (**c**), and heatmap showing top 15 differentially regulated genes within the Ca^{2+} signaling pathway (**d**) between COG P9906 BALL patients with 100% activated NK (n=85) or 100% resting NK (n=73) cells. Exact p-values were calculated in GSEA.

Figure S14: *NK cell phenotype and functions are similarly altered in pediatric and adult ALL*

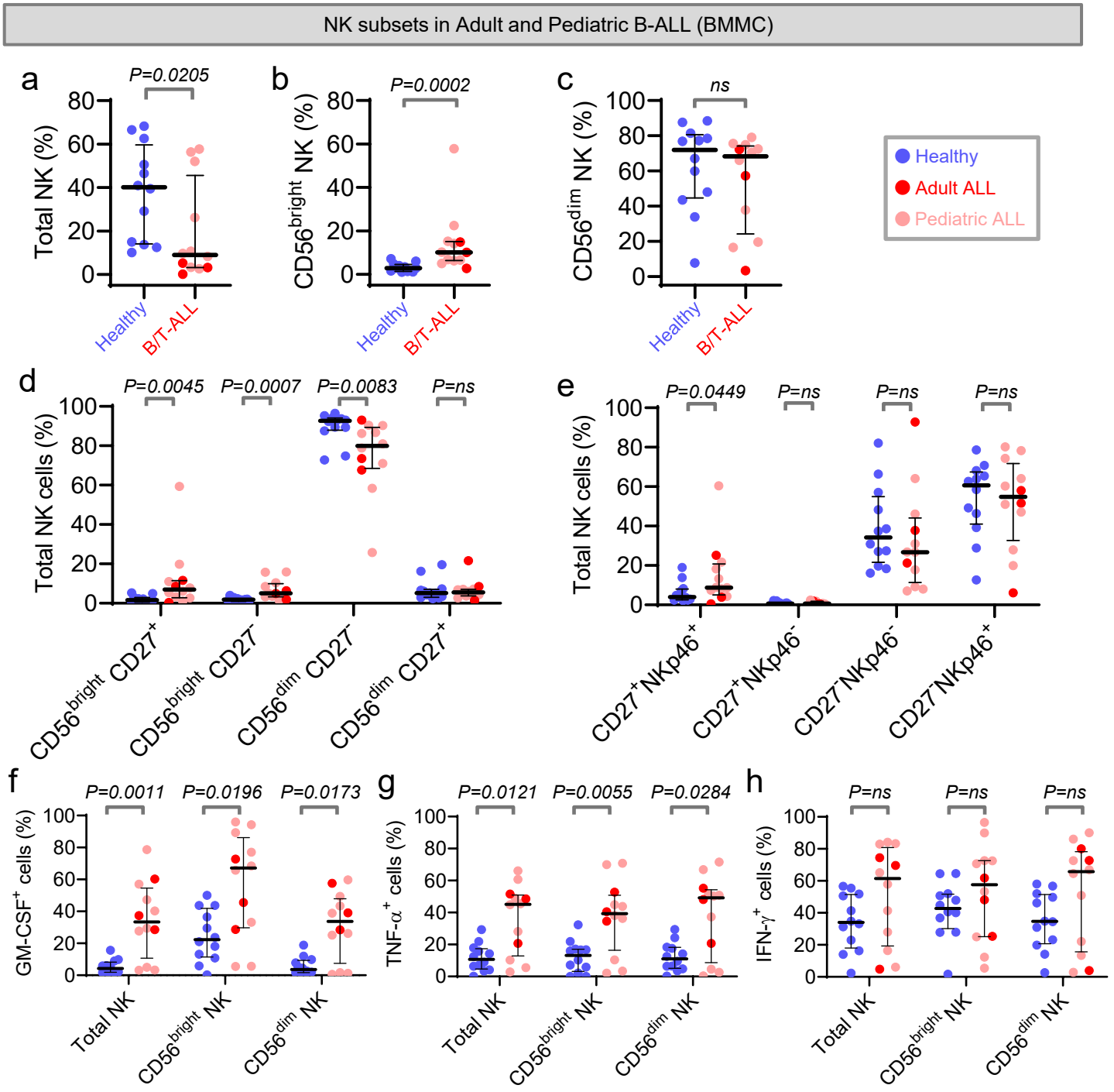

Figure S14: NK cell phenotype and functions are similarly altered in pediatric and adult ALL. (**a-e**) Comparison by CyTOF analysis of the frequencies of unstimulated NK cell subsets in BMMC from healthy controls (n=12), pediatric B/T-ALL (n=9) and adult B/T-ALL (n=3). Total NK cells as non-monocytes, non-T, non-B, $CD56^+$ cells (**a**); $CD56^{bright}$ (**b**) and $CD56^{dim}$ NK (**c**) subsets; $CD56^{bright}CD27^+$, $CD56^{bright}CD27^-$, $CD56^{dim}CD27^-$, $CD56^{dim}CD27^+$ NK fractions (**d**) ; and $CD27^+NKp46^+$, $CD27^+NKp46^-$, $CD27^-NKp46^-$, $CD27^-NKp46^+$ NK fractions (**e**). (**f-g**) Comparison by CyTOF analysis of the frequencies of GM-CSF^+ (**f**) , TNF-α^+ (**g**) , and IFN-γ^+ (**h**) NK cell subsets in BMMC from healthy controls (n=12), pediatric B/T-ALL (n=9) and adult B/T-ALL (n=3) after stimulation by PMA/Ionomycin for 4 hours. Graphs show median ± interquartile range. Exact p-values were calculated using Mann-Whitney test, ns=not significant.

Table S1: *List of high-risk B-ALL and T-ALL patient samples used in the study*

Patient ID	ALL subtype	Age	Sex	Tissue Type	Cytogenetics	Translocation /Mutation status	Disease status	Assay	Source
128	B-ALL	9.5	M	BMMC	46,XY,+5,-(9)(p),-13[14]/46,XY[6]	*CDKN2A* homozygous deletion (9p-/-)	Diagnosis	CyTOF	Stanford
227	B-ALL	4.9	M	BMMC	Normal, 46,XY male karyotype	Normal	Diagnosis	CyTOF	Stanford
268	B-ALL	12.1	M	BMMC	47~48,XY,+5,+mar[cp3]/46,XY[18]	Trisomy 5 clone observed	Diagnosis	CyTOF	Stanford
334	T-ALL	17.3	M	BMMC	46,XY,t(10;11)(p12;q14),del(12)(p11.2)[22]	*t(10;11) KMT2A* translocation	Diagnosis	CyTOF	Stanford
367	B-ALL	17.9	M	BMMC	46,XY,del(6)(q13q21),del(7)(p13p15)[9]/46,XY[11]	*IGH* rearrangement *(t14q32), CRLF2* overexpression, Ph-like	Diagnosis	CyTOF	Stanford
393	B-ALL	17.9	M	BMMC	Normal, 46,XY male karyotype	Normal	Diagnosis	CyTOF	Stanford
552	T-ALL	15.8	F	BMMC	45,XX,del(1)(p34~36),del(9)(p12),add(10)(p11.2),-11,del(11)(q),-14, add(16)(p13),+mar[cp20]	Unknown	Diagnosis	CyTOF	Stanford
718	Burkitt's B cell lymphoma	14.1	F	BMMC	46,XX,del(6)(q21),t(8;14)(q24;q32),del(9)(q13q22)[14]/46,XX[10]	*t(8;14)*-mediated MYC rearrangement	Diagnosis	CyTOF	Stanford
3277	T-ALL	12.6	F	BMMC	45,XX,der(8)t(8;14)(q24;q11.2),-14[2]/46,XX[20]	*der(8)t(8;14)*	Diagnosis	CyTOF	Stanford
6043	T-ALL	37	M	BMMC	Unknown	*NOTCH1* mutation	Diagnosis	CyTOF	UPENN
6457	B-ALL	62	F	BMMC	Unknown	*KMT2A*	Diagnosis	CyTOF	UPENN
6487	T-ALL	72	M	BMMC	45,X,-Y[8]/46,XY[6]	*NOTCH1* mutation	Diagnosis	CyTOF	UPENN
18067-HTB19-222	B-ALL	24	M	BMMC	Unknown	*JAK2(G); JAK2(S)*	Diagnosis	CyTOF	City of Hope

Table S1 contd.: *List of high-risk B-ALL and T-ALL patient samples used in the study*

Patient ID	ALL subtype	Age	Sex	Tissue Type	Cytogenetics	Translocation /Mutation status	Disease status	Assay	Source
65	B-ALL	33	F	PBMC	47 - 48, xx, -4-11, +3-4 probable t(4;11)	*t(4;11) KMT2A* translocation	Diagnosis	CyTOF	UPENN
779	B-ALL	48	F	PBMC	46,XX,t(1;11)(p32;q23)[10]/48,idem,+X,+21[10]/fish for *KMT2A* split pos 163/200 cells/fish for bcr-abl neg	*t(1;11) KMT2A* translocation	Diagnosis	CyTOF	UPENN
810	B-ALL	62	M	PBMC	46,XY[25]	Unknown	Diagnosis	CyTOF / Flow cytometry	UPENN
2142	B-ALL	30	M	PBMC	46,XY,del(9)(p21p21)[6]/46,XY[24]	Ph-like	Diagnosis	CyTOF	UPENN
3113	B-ALL	44	F	PBMC	Unknown	*KMT2A/AFF1*	Diagnosis	CyTOF	UPENN
4986	B-ALL	41	M	PBMC	46,XY[5]	Ph-like	Diagnosis	CyTOF	UPENN
4988	B-ALL	61	F	PBMC	46,XX,del(7)(p11.2)[7]/46,XX[13]	Ph-like	Refractory	CyTOF	UPENN
5921	T-ALL	32	M	PBMC	46,XY[20]	*NOTCH1* mutation	Diagnosis	CyTOF	UPENN
6070	T-ALL	46	M	PBMC	Unknown	*NOTCH1* mutation	Diagnosis	CyTOF	UPENN
6851	T-ALL	50	F	PBMC	46,XX[7].ish(ABL1 amp,BCRx2)[1]	Unknown	Diagnosis	CyTOF	UPENN
18067-LTB18-544	B-ALL	24	M	PBMC	Unknown	*JAK2(G); JAK2(S)*	Diagnosis	CyTOF	UPENN
5385	T-ALL	79	F	PBMC	46,XX,ins(22;?)(p11.2;?)[14]/46,XX[6]	*NOTCH1* mutation	Diagnosis	Flow cytometry	UPENN
18067-HTB18-029	B-ALL	57	F	PBMC	Unknown	*JAK2(G); JAK2(S)* (Ph-like)	Diagnosis	NK cytotoxicity	City of Hope
18067-HTB19-1382	B-ALL	24	M	PBMC	Normal	*EZH2; ETV6; KMT2D*	Diagnosis	Flow cytometry	City of Hope
18067-LTB18-578	B-ALL	44	F	PBMC	Normal	*KMT2D*	Diagnosis	Flow cytometry	City of Hope

Table S1 contd.: *List of high-risk B-ALL and T-ALL patient samples used in the study*

Patient ID	ALL subtype	Age	Sex	Tissue Type	Cytogenetics	Translocation /Mutation status	Disease status	Assay	Source
18067-HTB19-048	B-ALL	20	F	PBMC	47,XX,+22[6]	*JAK2; JAK1* (Ph-like)	Diagnosis	NK cytotoxicity, Calcium Flux, Flow cytometry	City of Hope
18067-HTB19-937	B-ALL	41	F	PBMC	46,XX[16].ish t(X;14)(p22.33; q32.33)(5'IGH+ ;3'IGH+)[2]	*IKZF1; JAK2(G); JAK2(S);PAX5* (Ph-like)	Diagnosis	Calcium Flux, Flow cytometry	City of Hope
18067-HTB19-001	B-ALL	35	F	PBMC	47,XX,+X[9]	*JAK2; NRAS* (Ph-like)	Diagnosis	Calcium Flux, Flow cytometry	City of Hope
18067-HTB19-376	B-ALL	30	F	PBMC	Unknown	*KMT2D*	Diagnosis	Calcium Flux	City of Hope
18067-LTB18-010	B-ALL	20	F	PBMC	50,XX,+X,+2,+ 4,t(9;22)(q34.1; q11.2),+der(22) t(9;22)[4]	Hi Risk, no Mutations	Diagnosis	Flow cytometry	City of Hope
18067-HTB19-289	B-ALL	43	F	PBMC	47,XX,- 2,t(3;15)(p23;q 15),del(5)(q22q 3?3),del(7)(p13 p15), +del(9)(p21.2), der(9)del(9)(p1 3p22)del(9)(q2 2)x2, der(10)t(2;10)(q21;q26),del(1 2)(p11.2p13.3), add(17)(q25)x2 ,- 20,+21,+mar[1 7]	*KRAS; KMT2D; PAX5*	Diagnosis	Flow cytometry	City of Hope
18067-LTB18-544	B-ALL	24	M	PBMC	47,XY,+X[6]	*JAK2(G); JAK2(S)* (Ph-like)	Diagnosis	Calcium Flux	City of Hope
18067-HTB19-1420	B-ALL	54	F	PBMC	46,XX,t(9;22)(q 34.1;q11.2)[6]; 48,sl,+4,- 16,+21,der(22)t (9;22) add (9)(q34.3),+der (22)t(9;22) add (9)[11] 47,sdl1,t(5;12)(q33;q13),- 21[3]	*KMT2C*	Diagnosis	NK cytotoxicity	City of Hope

Table S2: *Antibodies used for CyTOF immunophenotyping (Panel 1)*

Metal label	Target	Clone	Source	Concentration (μg/mL)	Titre (μg/mL)
113In	CD57	HNK1	Custom, Biolegend	265	2.5
141Pr	HLA-DR	L243	Custom, Biolegend	425	2
142Nd	CD19	HIB19	Fluidigm	500	5
145Nd	CD4	RPA-T4	Fluidigm	500	5
146Nd	CD8	RPA-T8	Fluidigm	500	5
147Sm	CD20	2H7	Fluidigm	500	5
149Sm	CTLA-4	14D3	Custom, eBioscience	510	5
150Nd	MIP-1β	D21-1351	Fluidigm	500	5
151Eu	CD107a	H4A3	Fluidigm	500	5
152Sm	TNF-α	Mab11	Fluidigm	500	5
153Eu	CD45RA	HI100	Fluidigm	500	5
154Sm	CD3	UCHT1	Fluidigm	500	5
158Gd	CD33	WM53	Fluidigm	500	5
159Tb	GM-CSF	BVD2-21C11	Fluidigm	500	5
160Gd	CD14	M5E2	Fluidigm	500	5
161Dy	IFN-γ	4S.B3	Custom, Biolegend	660	2.5
162Dy	NKp46	BAB281	Fluidigm	500	5
166Er	IL-2	MQ1-17h12	Fluidigm	500	5
167Er	CD27	L128	Fluidigm	500	5
170Er	PD1	EH12.1, BD	Fluidigm	500	2.5
171Yb	Granzyme B	GB11	Fluidigm	500	5
172Yb	PD-L2	24F.10C12	Fluidigm	500	5
173Yb	Perforin	B-D48	Custom, Abcam	500	2.5
175Lu	PD-L1	29E.2A3	Fluidigm	500	5
176Yb	CD56	NCAM16.2	Fluidigm	500	5
209Bi	CD16	3G8	Fluidigm	500	5

Table S3: *Antibodies used for CyTOF immunophenotyping (Panel 2)*

Metal label	Target	Clone	Source	Concentration (μg/mL)	Titre (μg/mL)
113In	CD57	HNK1	Custom, Biolegend	265	2.5
141Pr	HLA-DR	L243	Custom, Biolegend	425	2
142Nd	CD19	HIB19	Fluidigm	500	5
145Nd	CD4	RPA-T4	Fluidigm	500	5
146Nd	CD8	RPA-T8	Fluidigm	500	5
147Sm	CD20	2H7	Fluidigm	500	5
148Nd	ICOS	C398.4A	Fluidigm	500	5
149Sm	CTLA-4	14D3	Custom, eBioscience	510	5
152Sm	TNF-α	Mab11	Fluidigm	500	5
153Eu	TIGIT	MBSA43	Fluidigm	500	5
154Sm	CD3	UCHT1	Fluidigm	500	5
157Gd	ILT2	GHI/75	Custom, Biolengend	460	5
158Gd	CD33	WM53	Fluidigm	500	5
159Tb	GM-CSF	BVD2-21C11	Fluidigm	500	5
160Gd	CD14	M5E2	Fluidigm	500	5
161Dy	IFN-γ	4S.B3	Custom, Biolegend	660	2.5
162Dy	NKp46	BAB281	Fluidigm	500	5
163Dy	Siglec-7	6-434	Custom, Biolegend	215	2
164Dy	KLRG1	SA231A2	Custom, Biolegend	445	2
165Ho	LAG-3	11C3C65	Fluidigm	500	5
167Er	CD27	L128	Fluidigm	500	5
168Er	Ki-67	B56	Fluidigm	500	5
169Tm	TIM-3	F38-2E2	Fluidigm	500	5
170Er	PD1	EH12.1, BD	Fluidigm	500	2.5
172Yb	PD-L2	24F.10C12	Fluidigm	500	5
175Lu	PD-L1	29E.2A3	Fluidigm	500	5
176Yb	CD56	NCAM16.2	Fluidigm	500	5
209Bi	CD16	3G8	Fluidigm	500	5

Table S4: *Reagents and antibodies used for flow cytometry*

Name	Fluorophore	Clone	Dilution/ Concentration	Source
Anti-human CD3	FITC	UCHT1	1:100	Biolegend
Anti-human CD56	APC	5.1H11	1:100	Biolegend
Anti-human CD45	PerCP/FITC	2D1	1:100	Biolegend
Anti-human CD94	PECY7	DX22	1:100	Biolegend
Anti-human NKp44	PE	P44-8	1:100	Biolegend
Anti-human CD62L	PECY5	DREG-56	1:100	Biolegend
Anti-human DNAM-1	BV605	11A8	1:100	Biolegend
Anti-human CD11b	APC-R700	M1/70	1:100	BD
Anti-human CD27	PE	M-T271	3:100	BD
Anti-human CD16	BV711	3G8	1:100	BD
Anti-human CD158a	BV421	HP-3E4	1:100	BD
Anti-human NKG2A	BV605	131411	1:100	BD
Anti-human NKp30	BV750	P30-15	1:100	BD
Anti-human CD56	BV510	NCAM16.2	1:100	BD
Anti-human CD3	BUV805	UCHT1	1:100	BD
Anti-human CD69	BUV737	FN50	1:100	BD
Anti-human CD19	BUV661	HIB19	1:100	BD
Anti-human CD14	BUV395	M5E2	1:100	BD
Ghost-Dye UV450	NA	NA	1:100	Tonbo Biosciences
Indo-AM	NA	NA	1.5μM	ThermoFisher Scientific
7AAD	NA	NA	1:100	Biolegend
DAPI	NA	NA	300nM	Biolegend

Table S5: *Number of NK cell events acquired by CyTOF and flow cytometry*

Sample Name	Tissue	ALL subtype	Assay	Unstimulated NK cell events	Stimulated NK cell events
128	BMMC	B-ALL	CyTOF	4346	3512
227	BMMC	B-ALL	CyTOF	2899	2571
268	BMMC	B-ALL	CyTOF	327	328
367	BMMC	B-ALL	CyTOF	10242	10918
393	BMMC	B-ALL	CyTOF	1847	1733
718	BMMC	Burkitt's B cell lymphoma	CyTOF	989	855
6457	BMMC	B-ALL	CyTOF	289	282
18067-HTB19-222	BMMC	B-ALL	CyTOF	852	2284
334	BMMC	T-ALL	CyTOF	15189	11964
552	BMMC	T-ALL	CyTOF	4016	4667
3277	BMMC	T-ALL	CyTOF	10001	9702
6043	BMMC	T-ALL	CyTOF	1783	1463
6487	BMMC	T-ALL	CyTOF	31503	36981
65	PBMC	B-ALL	CyTOF	625	540
779	PBMC	B-ALL	CyTOF	1511	1461
810	PBMC	B-ALL	CyTOF	1356	6584
2142	PBMC	B-ALL	CyTOF	3760	3149
3113	PBMC	B-ALL	CyTOF	3577	3167
4986	PBMC	B-ALL	CyTOF	2150	2150
4988	PBMC	B-ALL	CyTOF	2315	2249
18067-LTB18-544	PBMC	B-ALL	CyTOF	1500	1855
5921	PBMC	T-ALL	CyTOF	2513	2812
6070	PBMC	T-ALL	CyTOF	3425	3377
6851	PBMC	T-ALL	CyTOF	14617	1477
18067-LTB18-010	PBMC	B-ALL	Flow Cytometry	4487	NA
18067-HTB19-289	PBMC	B-ALL	Flow Cytometry	195	NA
18067-LTB18-578	PBMC	B-ALL	Flow Cytometry	4324	NA
18067-HTB19-001	PBMC	B-ALL	Flow Cytometry	2233	NA
18067-HTB19-1382	PBMC	B-ALL	Flow Cytometry	3019	NA
18067-HTB19-048	PBMC	B-ALL	Flow Cytometry	3412	NA
18067-HTB19-937	PBMC	B-ALL	Flow Cytometry	4881	NA
810	PBMC	B-ALL	Flow Cytometry	3152	NA
5385	PBMC	T-ALL	Flow Cytometry	1715	NA